Design Of a Photocatalytic Reaction System for Pollutant Degradation: A Computational Study

Fatima Aamir, Muhammad Suleman Tahir, Abdul Basit, Abdul Hannan Zahid
[1]Department of Chemical Engineering, University of Gujrat, Pakistan
***Correspondence:** fatimaaamirabbas966@gmail.com

Citation | Aamir. F, Tahir. M. S, Basit. A, Zahid. A. H, "Design of A Photocatalytic Reaction System for Pollutant Degradation: A Computational Study", IJIST, Special Issue. pp 245-256, March 2025.
Received | Feb 25, 2025 **Revised |** March 09, 2025 **Accepted |** March 15, 2025 **Published |** March 18, 2025.

In this study, Computational Fluid Dynamics (CFD) was used to model and simulate the photocatalytic degradation of methyl orange (MeO) in a stirred photoreactor, particularly in the presence of a bismuth oxide catalyst. This approach not only provides an effective method for treating wastewater by breaking down harmful dye pollutants but also highlights the potential of cost-effective and eco-friendly catalytic materials for environmental cleanup. In the first phase, the catalyst was evenly distributed in an aqueous MeO solution, where photocatalysis was employed to degrade the pollutant. The structural properties of the catalyst were analyzed using scanning electron microscopy (SEM). Experiments were conducted to examine how different factors, such as pH and pollutant concentration, influenced MeO removal.

In the next step, CFD was used to numerically analyze MeO degradation through photocatalysis. The results showed that the photoreactor effectively broke down MeO. CFD modeling further explained the degradation mechanism, revealing that hydroxyl radicals (OH•) played a key role in the heterogeneous photocatalytic process. Photocatalysis significantly contributed to pollutant breakdown in both experimental and simulated phases.

The CFD models closely matched experimental data, confirming the findings related to fluid dynamics and species concentration. By offering deeper insights into mass transfer and reaction kinetics at a fraction of the cost and time, CFD proved to be more efficient than experimental methods in analyzing MeO degradation.

Keywords. Computational Fluid Dynamics (CFD); Photocatalytic Degradation; Methyl Orange; Bi_2O_3 Nanoparticles; Predictive Modelling

Introduction:

Environmental pollution is a long-standing issue and a major cause of environmental illness and mortality, making it one of the biggest challenges facing humanity today. Every day, our environment is increasingly contaminated by various toxic and hazardous pollutants. Among these, organic pollutants such as pesticides[1], pharmaceuticals[2], and dyes[3] are particularly concerning due to their harmful effects on human health and aquatic life.

Methyl orange, a synthetic dye widely used in textiles, printing, and laboratories, is one such pollutant that requires degradation. Due to its chemical properties, it poses serious health and environmental risks to living organisms. Pollutant degradation refers to breaking down or removing harmful substances. The available methods for degradation fall into three main categories: physical, chemical, and biological. Physical methods include filtration and adsorption, chemical methods involve advanced oxidation processes[4], electrochemical techniques[5], and chemical precipitation, while biological methods include bioremediation[6], phytoremediation[7], and enzymatic treatment[8]. The conventional techniques for degrading organic contaminants may eventually be replaced by the environmentally friendly approach of photocatalysis.

Photocatalysis is considered one of the most effective chemical methods due to its high efficiency in breaking down persistent pollutants, eco-friendly nature, low-cost catalyst materials, self-sustaining mechanism, and scalability. This technique is particularly useful for treating wastewater with high contaminant levels, limited biodegradability, and complex compositions[9]. In practical applications, photocatalysts use solar energy to break down pollutants[10], degrading organic contaminants by absorbing specific wavelengths of light in water[11][12]. Under ambient temperature and pressure, photocatalysis converts pollutants into harmless molecules through redox reactions[13][14].

However, some photocatalysts face limitations, including high band gap energies (Eg), low light absorption capacity, and rapid electron-hole recombination. A high Eg value leads to inefficient charge separation, requiring more energy for activation[15]. Additionally, electrons and holes may recombine before contributing to the photocatalytic process, reducing the generation of reactive oxygen species (ROS) needed for complete photodegradation. This fast recombination rate hinders overall quantum efficiency[16].

Despite these challenges, photocatalysis remains one of the most effective techniques. The process begins when hydroxyl radicals (·OH) attack the dye molecule's weakest chemical bonds, such as the azo bond (–N=N–). When this structure is broken, the dye's conjugated system is disrupted[17]. As the reaction progresses, the intermediates undergo further oxidation, ultimately decomposing into carbon dioxide and water[18].

Table 1 Reactions included in the degradation process[19]

Reactions
$2HO_2 \rightarrow O_2^{\circ} + H_2O_2$
$H_2O_2 + O_2^{\circ} \rightarrow OH^{\circ} + OH^{-} + O_2$
$e^{-} + O_2 \rightarrow O_2^{\circ-}$
$O_2^{\circ-} + H^{+} \rightarrow 2HO^{\circ}{}_2$

The reactivity of dyes in degradation systems depends on their chemical structure[20]. Complex dyes generally have low photodegradability due to the presence of functional groups that affect adsorption characteristics. Many researchers are studying the removal of different dyes under visible and UV radiation[21][22].

Experimental work often involves multiple trials and errors, requiring extensive time and effort while sometimes yielding ineffective results. One of the most efficient ways to overcome these limitations is through modeling and simulation[23]. Computational Fluid Dynamics (CFD) simulations help analyze fluid behavior under different conditions, such as

flow dynamics and heat transfer. CFD also solves governing equations that describe fluid flow and decomposes the physical domain into smaller parts (meshing), including:

1. **Navier-Stokes equations** – govern the flow of viscous fluids.
2. **Continuity equation** – ensures mass conservation.
3. **Energy equation** – explains heat transfer within a fluid.

There is growing recognition of CFD's potential in chemical engineering and reaction engineering[24]. It has also been applied in various fields, such as fluidization[25] and multiphase flow systems[26].

Simulation methods include the Finite Volume Method (FVM), Finite Difference Method (FDM), Finite Element Method (FEM), and Lattice Boltzmann Method (LBM)[27]. Among these, FVM is the most accurate, particularly for processes involving interspecies interactions.

Research Objectives:

This paper presents the design of a photocatalytic reactor using advanced modeling and simulation methods for pollutant degradation through heterogeneous photocatalysis.

The primary objective of this research is to develop a Computational Fluid Dynamics (CFD) model in ANSYS Fluent to simulate the photocatalytic breakdown of wastewater contaminants using a bismuth oxide catalyst effectively. Additionally, this study aims to analyze how contaminant concentration and photocatalyst dosage influence the efficiency of pollutant degradation in an environmentally friendly manner.

Novelty statement:

This study provides mechanistic insights by modeling and simulating the photocatalytic degradation of methyl orange (MeO) in a stirred photoreactor using Computational Fluid Dynamics (CFD), particularly with a bismuth oxide catalyst. This approach not only offers an efficient method for treating wastewater by breaking down harmful dye contaminants but also highlights the potential of cost-effective and eco-friendly catalytic materials for environmental remediation.

Material and Methods:

The experimental procedure is detailed here, with all chemicals used in the preparation process being of AR grade and purchased from Merck. Double-distilled (DD) water was used throughout. $Bi(NO_3)_3 \cdot 5H_2O$ was dissolved in a few drops of HNO_3 and diluted to a 0.1 M solution with DD water to prevent Bi ion precipitation. After adding NH_4OH dropwise, the resulting gel was filtered and washed with DD water. The gel was then refluxed at 80°C for four hours to form crystals.

To convert $Bi(OH)_3$ into its oxide form, it was calcined at 600°C for three hours. The structural, optical, and degradation characteristics of the oxide sample were analyzed to determine its crystal system, band gap, and reaction kinetics. Polymorph alpha-bismuth oxide was synthesized using a simple, surfactant-free chemical process, with methyl orange (MeO) used as a model pollutant to assess its degradation properties. MeO, a water-soluble azo dye, was chosen with an initial concentration of 16.4 mg/L and a solution pH of 7.07.

For photocatalysis, a 500W Xenon lamp (Wacom XDS501S) was used as the light source due to its high intensity, ensuring strong photon flux, faster reaction rates, and efficient charge carrier activity. Bismuth oxide, as a catalyst, has a band gap that allows it to absorb visible light from the xenon lamp, enhancing absorption and improving degradation efficiency. The experiment was conducted 47 cm from the light source, with an incident light intensity of 17,400 lux on the sample. Dye colorization kinetics were monitored at intervals of one to four hours using a UV-vis spectrophotometer (Techcomp UV2301) to measure the residual dye concentration in the solution.

Initially, Bi_2O_3 was dispersed in the MeO aqueous solution and stirred in the dark for an hour, showing only a slight decrease in absorption. The photocatalytic experiment was conducted under two conditions: (i) without photocatalyst light irradiation and (ii) with photocatalyst irradiation. Results indicated that a portion of the MeO molecules adsorbed onto the sample's surface. Upon light exposure, the optimal absorption gradually decreased as irradiation time increased, confirming the catalytic oxidation of MeO by Bi_2O_3. The MeO absorption band shifted from 464 nm to 452 nm, indicating a stepwise movement of ethyl groups under radiation.

Table 2 Some chemical and physical properties of MeO

Chemical Name	**Dye Type**	**Molecular Weight g/mol**	**Molecular Formula**
4- [4(Dimethyl Amino) phenyl azo] Benzene Sulfonic Acid Sodium salt	Organic	327.33	$C_{14}H_{14}N_3NaO_3S$

Analytical Techniques:

The ultraviolet-visible (UV-Vis) spectrum recorded during the photodegradation of MeO with Bi_2O_3 is shown in Figure. 1. MeO has a maximum absorption at 464 nm and can absorb light in both the visible and ultraviolet regions. The absorption in the visible spectrum is attributed to MeO's azo linkage chromophore.

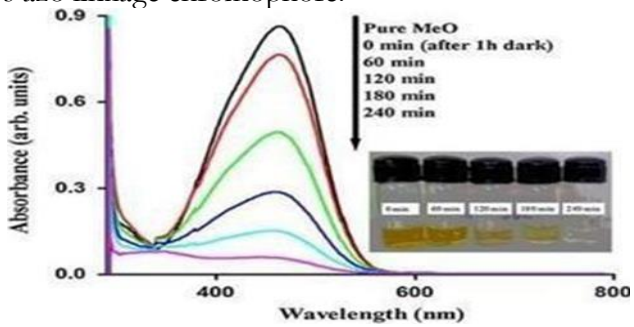

Figure 1. UV-vis spectra of photocatalytic degradation of MeO using Bi_2O_3 calcined at 600°C[28]

Figure. 2 (HR-SEM) presents an image used to analyze the surface morphology of the Bi_2O_3 catalyst. The sample consists of irregularly shaped platelets of varying sizes and forms, with some appearing as large, smooth platelets with sharp edges. This analysis provides insights into the textural properties of the catalyst, including porosity, particle size, and surface roughness—key factors influencing its performance and activity. HR-SEM is crucial as it captures high-magnification images, revealing nanoscale features such as particle size distribution, surface morphology, and structural integrity, all of which impact the material's physical, chemical, and catalytic properties.

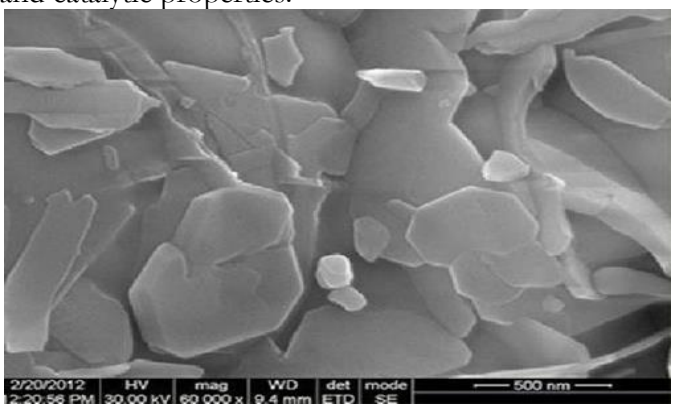

Figure 2. HR-SEM images of Bi_2O_3 calcined at 600°C [28]

Properties and the Degradation Mechanism of Photocatalysis

The photocatalytic process involves a reactor equipped with a steel mixer/stirrer, an inlet zone, a light source, and an outlet zone. The reacting mixture is placed inside the reactor, with bismuth oxide (Bi_2O_3) dispersed as the catalyst. A 500W lamp serves as the ultraviolet light source, maintaining a constant intensity throughout the experiment.

A 50 ml dye solution is introduced into the reactor, and the catalyst is dispersed within it. When Bi_2O_3 is mixed with the MeO aqueous solution in the dark and stirred for an hour, only a slight reduction in absorption is observed. However, after four hours of exposure to light, the degradation of MeO without a photocatalyst is just 2%, whereas with Bi_2O_3, it reaches 93%. This confirms that Bi_2O_3 significantly enhances the decolorization of MeO. Following four hours of irradiation, the initial MeO concentration decreases from 16.4 mg/L to 1.1 mg/L. Samples were collected at specific intervals for analysis.

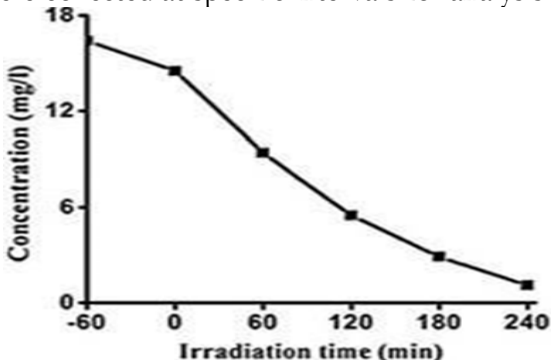

Figure 3. Variation in Concentration of pollutants with time in the degradation process [28]

CFD Modelling:

Governing Equations:

The equations for mass balance, momentum, and continuity for each species involved are presented in Equations (1)– (3) below. By solving these equations, the mass fraction, velocity, and pressure contours can be determined.

$$\frac{\partial(\alpha q \rho q)}{\partial t} + \nabla.(\alpha q \rho q u q) = \sum_{\rho=1}^{n} mp\dot{q} \quad (1)$$

$$\frac{\partial(\alpha q \rho q u q)}{\partial t} + \nabla.(\alpha q \rho q u q u q) = -\alpha q \nabla \rho + \alpha q \rho q g + \nabla.\tau q + \sum_{p=1}^{n}(Rpq + mpquq) + \alpha q \rho q(F_q + F_{lift,q} + F_{vm,q}) \quad (2)$$

$$\frac{\partial}{\partial t}(\alpha i \rho i Y i q) + \nabla.(\alpha i \rho i u i q) = -\nabla.\alpha i J i q + \alpha i R i q + \alpha i S i q + \sum_{p=1}^{n}(mpqij - mijpq) \quad (3)$$

u, ρ, Y, and α are the velocity, density mass fraction, and volume fraction of phases. For all the reactions, Arrhenius's reaction rate has been consumed.

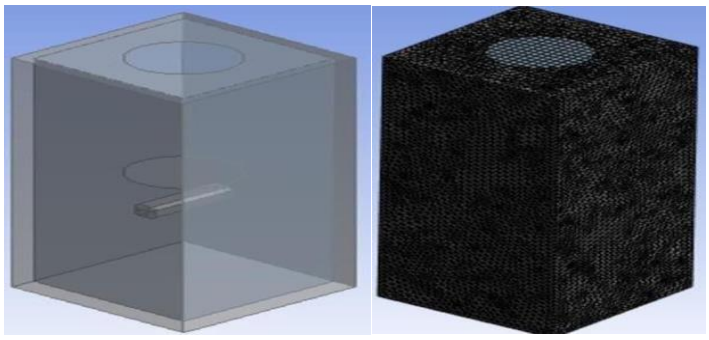

Figure 4 Geometry and meshing of the stirred photoreactor used in the degradation process

Boundary Conditions:

Boundary conditions play a crucial role in computational fluid dynamics (CFD) simulations, as they define fluid interactions with the surroundings and influence the

simulation's accuracy, stability, and realism. The photoreactor has four side walls, modeled as rigid solids with a no-slip boundary condition applied to their surfaces.

As shown in Figure. 4, turbulence and eddies significantly impact the process due to the presence of the stirrer. To capture these effects accurately, the k-ε turbulence model is used, providing reliable results that align with practical observations [29]. The photoreactor contains a 50 mL solution, and the initial values of various parameters, such as interior velocity, are set accordingly. A no-slip condition is applied to the four side walls.

A hollow space exists above the stirrer, allowing the reactant mixture to be introduced into the reactor. During the process, turbulence and eddies play a crucial role due to the stirrer's motion. Therefore, the k-ε turbulence model is implemented to ensure accurate and trustworthy results [30].

Numerical Method:

The photoreactor was designed using ANSYS Design Modeler. After modeling, meshing, and solving the continuity, momentum, and mass balance equations, ANSYS Fluent software was used. The software employs a finite volume approach, and the pressure-based solver was chosen due to its suitability for incompressible fluids and unstable-state equations.

For numerical stability and convergence, transient equations were discretized using the implicit first-order technique. Velocity, pressure, and species mole fractions were stored at nodes using a node-based solving method. The SIMPLE algorithm was used to couple velocity and pressure variables, while Green-Gauss discretization was applied to diffusion terms for practicality [31]. Standard wall functions were selected as the near-wall treatment approach, and mesh refinement near the walls ensured accurate flow field resolution.

A moving reference frame (MRF) technique was implemented to simulate the stirred tank photoreactor. The computational domain was divided into two zones: one containing the stirrer and another for the rest of the reactor. Instead of mobilizing the stirrer, a rotating motion was imposed on the inner zone to simulate fluid motion efficiently [32].

The discretized equations were solved for each mesh element, making mesh size crucial for accuracy. A grid independence study was conducted to determine the optimal mesh size. The simulation was transient, performed using ANSYS Fluent, with a time step size of 10 minutes and a total of 14,400 steps. The simulation ran for over two hours to generate results for post-processing. The minimum processor required for such simulations was an Intel Core i5 series.

Table 3. Mesh independence analysis

Reactor	Case	Mesh Sizes	No. of elements
	1	80cm	21841
Stirred-photoreactor	2	60cm	37324
	3	40cm	108273

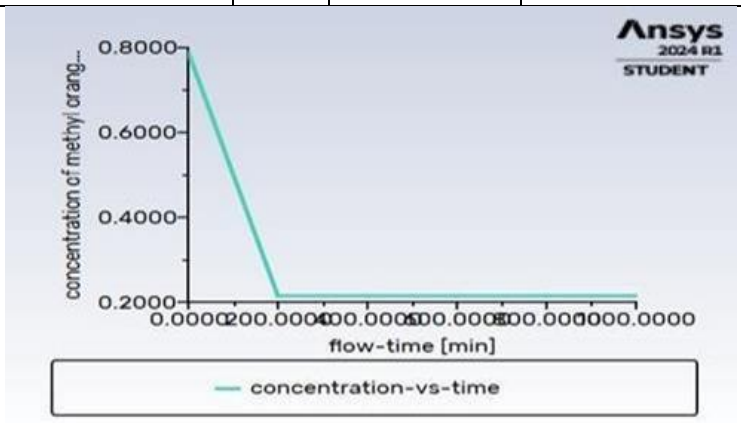

Figure 5. Trend of decreasing concentration of MeO pollutant concerning time.

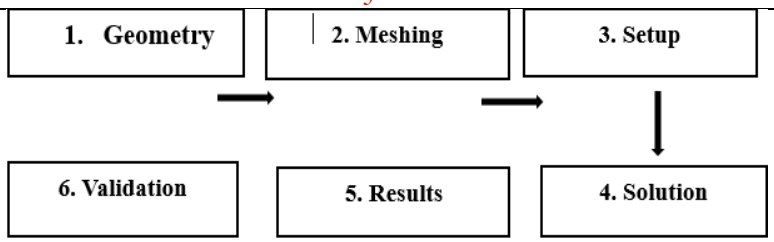

Figure 6. Flow diagram of methodology of the process used for the degradation in CFD simulation

SEM and AFM Analysis Results:

SEM results for the catalyst surface were analyzed using high-resolution images, as shown in Figure. 2. The Bi_2O_3 sample appears as irregularly shaped platelets of varying sizes and forms. Below, larger, smooth platelets with sharp edges can be observed.

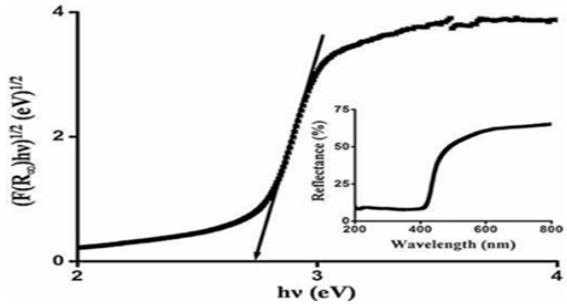

Figure 7. Band gap of Bi_2O_3 calcined at 600°C using Kubelka- Munk function with the reflectance spectra as the inset[28]

Figure. 7 presents the bandgap of Bi_2O_3 along with its reflectance spectra in the inset. The Kubelka-Munk function is applied to the reflectance spectrum to determine the sample's bandgap.

$$K/S = (1-R_\infty)^2/2R_\infty \equiv F(R_\infty) \quad (4)$$

Kubelka-Munk absorption (K) and scattering (S) coefficients are used to analyze the optical properties of Bi_2O_3. The Kubelka-Munk function, $F(R_\infty)$, is defined as $F(R_\infty) = (K/S)$, where R_∞ represents $R_{sample}/R_{standard}$. The band gap is determined by extrapolating the linear portion of the $(F(R_\infty)h\nu)^{1/2}$ vs. hν plot to $F(R_\infty) = 0$. The calculated bandgap value is 2.7344 eV (454 nm). This visible-light absorption suggests that Bi_2O_3 can act as a photocatalyst under visible light. MeO exhibits maximum absorption at 464 nm, covering both visible and ultraviolet regions, primarily due to its azo chromophore.

Results and Discussions:

CFD Results:

CFD simulations provide valuable insights into the spatial distribution of reactive species, such as •OH radicals, which are difficult to track experimentally in advanced oxidation processes (AOPs). The contours of velocity, velocity vectors, and mass concentration of pollutants help visualize the fluid dynamics within the photoreactor. Velocity vectors illustrate the flow patterns, showing how the fluid moves throughout the reactor. Dead zones, caused by eddies, indicate areas with reduced mixing, which can affect pollutant degradation efficiency. These simulations enable optimization of reactor design by identifying areas for improved fluid flow and mixing.

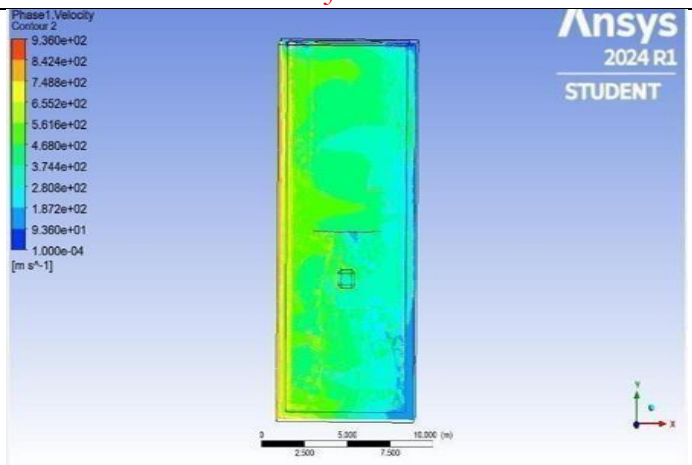

Figure 8. Contour of velocity used in the degradation process in the stirred photoreactor

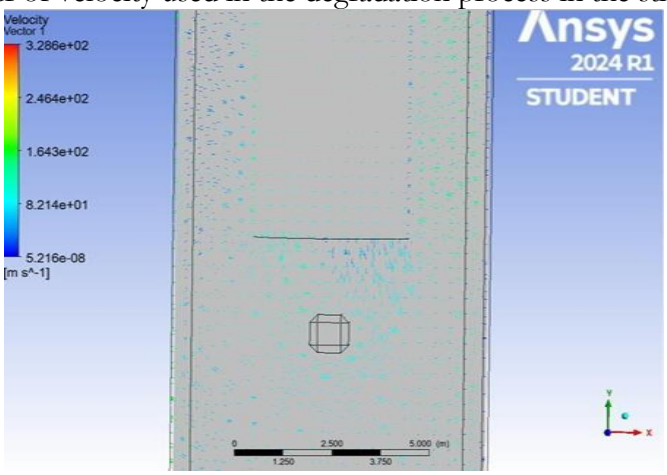

Figure 9. Velocity vectors of the stirred photoreactor of the degradation process

Yes, mass concentration contours are essential for understanding the spatial distribution of species within the reactor. They help in identifying regions with high and low concentrations, allowing researchers to pinpoint areas of pollutant accumulation or rapid degradation. This information is crucial for optimizing photocatalytic reactor design, ensuring uniform mixing, and enhancing reaction efficiency. By analyzing these contours, adjustments can be made to operating conditions, such as catalyst dosage, flow rates, or reactor geometry, to improve overall pollutant degradation performance.

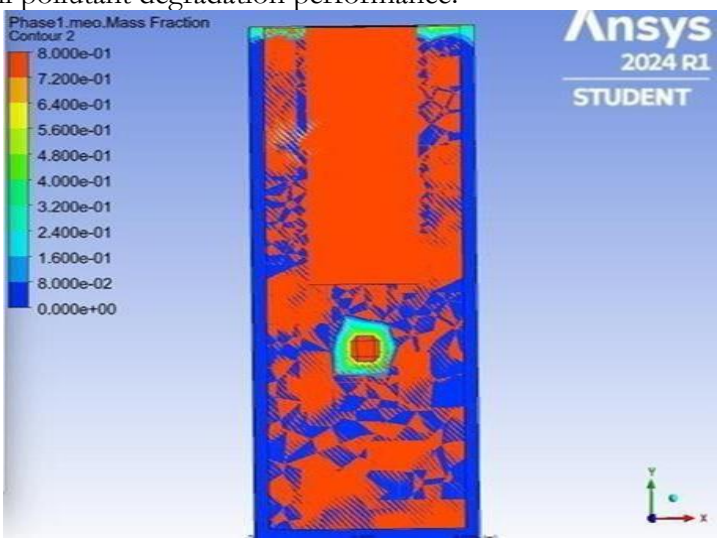

Figure 10. Mass concentration contour of the pollutant degraded in the stirred photoreactor

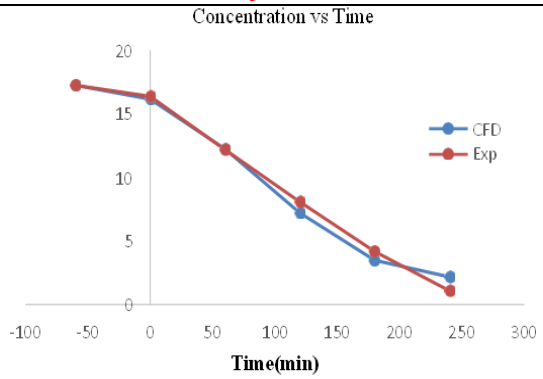

Figure 11. Comparison of CFD and experimental results of MeO degradation with time in the stirred-photo reactor

Yes, the high R^2 value (0.93) indicates strong agreement between the CFD model and experimental results, validating the accuracy of the simulation. The similarity in trends confirms that the model effectively captures the degradation kinetics of MeO. This suggests that CFD can reliably predict pollutant breakdown in photocatalytic reactors, making it a valuable tool for optimizing reaction conditions without extensive experimental trials.

Discussion:

Your conclusion effectively highlights the significance of Bi_2O_3 as a visible-light-driven photocatalyst and its potential for wastewater treatment. Here are some refinements for clarity and impact:

1. **Strengthen the Final Takeaway:** Conclude with a strong statement about Bi_2O_3's potential and future research directions.
2. **Improve Flow and Conciseness:** Some sections could be streamlined for readability.
3. **Enhance Technical Precision:** Differentiate between experimental and simulated findings when discussing mass transfer and turbulence.

Would you like me to refine and edit it accordingly?

Conclusion:

In this study, the removal of methyl orange (MeO) from wastewater was investigated due to its toxicity to aquatic life. Computational Fluid Dynamics (CFD) simulations were employed to model MeO degradation under heterogeneous photocatalytic conditions, incorporating the mixture model and radiation model. Key factors such as light intensity, catalyst distribution, and impeller speed were optimized to achieve maximum degradation. Experimental results confirmed significant pollutant removal, with approximately 93% efficiency. Numerical simulations provided insight into reaction mechanisms and concentration variations over time, validating the model's reliability. The strong agreement between CFD and experimental findings highlights CFD's potential to reduce experimental costs while optimizing wastewater treatment processes.

Limitations:

- The model needs to be .validated if the pollutant and catalyst are changed.

Future work:

Based on the conclusion provided, here are some potential future work conclusions:

- Investigate the scalability of the stirred photoreactor system using CFD for industrial applications while maintaining high removal efficiency.
- Extend the CFD simulations to include systems with multiple pollutants and evaluate their interactions and degradation pathways.
- Explore various methods of catalyst distribution to improve pollutant degradation efficiency further and validate these techniques through additional CFD simulations.

Acknowledgment: The authors wish to express their gratitude to the University of Gujrat for their invaluable contribution and support throughout this study. Sincere efforts from all participants were essential to the completion of this study, and they deserve special recognition. We also owe a debt of gratitude to our parents for their financial and moral assistance as well as prayers.

Author's Contribution: MST supervised the project and provided critical feedback during the research process. AB conceptualized the research idea designed the study framework and helps in performing computational modeling and simulation work. AHZ assisted with experimental data and monitored data acquisition. .

Conflict of interest: The authors declare that they have no known competing financial interests or personal relationships that could have appeared to influence the work reported in this paper.

Project details: Nil

References:

[1] P. S. Yuan Liu, Jian Wang , Xuran Zhu, Yang Liu, Ming Cheng, Weihai Xing, Yuping Wan, Na Li, Liting Yang, "Effects of electrolyzed water treatment on pesticide removal and texture quality in fresh-cut cabbage, broccoli, and color pepper," *Food Chem.*, vol. 353, p. 129408, 2021, doi: https://doi.org/10.1016/j.foodchem.2021.129408.

[2] R. A. T.-P. Ana L. Camargo-Perea, Efraím A. Serna-Galvis, Judy Lee, "Understanding the effects of mineral water matrix on degradation of several pharmaceuticals by ultrasound: Influence of chemical structure and concentration of the pollutants," *Ultrason. Sonochem.*, vol. 73, p. 105500, 2021, doi: https://doi.org/10.1016/j.ultsonch.2021.105500.

[3] C. A. Islam Ibrahim, George Belessiotis, Michalis K. Arfanis, "Surfactant Effects on the Synthesis of Redox Bifunctional V2O5 Photocatalysts," *Materials (Basel).*, vol. 13, no. 20, p. 4665, 2020, doi: 10.3390/ma13204665.

[4] A. B. R. Cátia Magro, Eduardo P. Mateus, Juan M. Paz-Garcia, "Emerging organic contaminants in wastewater: Understanding electrochemical reactors for triclosan and its by-products degradation," *Chemosphere*, vol. 247, p. 125758, 2020, doi: https://doi.org/10.1016/j.chemosphere.2019.125758.

[5] Luis Baptista-Pires , Norra Giannis-Florjan and Jelena Radjenovic, "Graphene-based sponges for electrochemical degradation of persistent organic contaminants," *Water Res.*, vol. 203, p. 117492, 2021, doi: https://doi.org/10.1016/j.watres.2021.117492.

[6] M. N. A. Rashi Miglani, Nagma Parveen, Ankit Kumar, Mohd. Arif Ansari, Soumya Khanna, Gaurav Rawat, Amrita Kumari Panda, Satpal Singh Bisht, Jyoti Upadhyay, "Degradation of Xenobiotic Pollutants: An Environmentally Sustainable Approach," *Metabolites*, vol. 12, no. 9, p. 818, 2022, doi: https://doi.org/10.3390/metabo12090818.

[7] O. O. B. Modupe Stella Ayilara, "Bioremediation of environmental wastes: the role of microorganisms," *Front. Agron.*, vol. 5, 2023, doi: 10.3389/fagro.2023.1183691.

[8] F. A. & S. S. A. Khadega A. Almaqdi, Rana Morsi, Bahia Alhayuti, "LC-MSMS based screening of emerging pollutant degradation by different peroxidases," *BMC Biotechnol.*, vol. 19, no. 83, 2019, doi: https://doi.org/10.1186/s12896-019-0574-y.

[9] R. A. El-Salamony, E. Amdeha, S. A. Ghoneim, N. A. Badawy, K. M. Salem, and A. M. Al-Sabagh, "Titania modified activated carbon prepared from sugarcane bagasse: adsorption and photocatalytic degradation of methylene blue under visible light irradiation," *Environ. Technol.*, vol. 38, no. 24, pp. 3122–3136, Dec. 2017, doi: 10.1080/21622515.2017.1290148.

[10] S. K. N.R. Khalid, A. Majid, M. Bilal Tahir, N.A. Niaz, "Carbonaceous-TiO2

nanomaterials for photocatalytic degradation of pollutants: A review," *Ceram. Int.*, vol. 43, no. 17, pp. 14552–14571, 2017, doi: https://doi.org/10.1016/j.ceramint.2017.08.143.

[11] W. T. C. Yean Ling Pang, Steven Lim, Hwai Chyuan Ong, "Synthesis, characteristics and sonocatalytic activities of calcined γ-Fe2O3 and TiO2 nanotubes/γ-Fe2O3 magnetic catalysts in the degradation of Orange G," *Ultrason. Sonochem.*, vol. 29, pp. 317–327, 2016, doi: https://doi.org/10.1016/j.ultsonch.2015.10.003.

[12] C. H. Hak, L. C. Sim, K. H. Leong, P. F. Lim, Y. H. Chin, and P. Saravanan, "M/g-C3N4 (M=Ag, Au, and Pd) composite: synthesis via sunlight photodeposition and application towards the degradation of bisphenol A," *Environ. Sci. Pollut. Res.*, vol. 25, no. 25, pp. 25401–25412, Sep. 2018, doi: 10.1007/S11356-018-2632-8/METRICS.

[13] K.-H. P. Wan-Kuen Jo, "Heterogeneous photocatalysis of aromatic and chlorinated volatile organic compounds (VOCs) for non-occupational indoor air application," *Chemosphere*, vol. 57, no. 7, pp. 555–565, 2004, doi: https://doi.org/10.1016/j.chemosphere.2004.08.018.

[14] W. Z. Kowarsk Beata, Jerzy Baron, Stanisław Kandefer, "Incineration of Municipal Sewage Sludge in a Fluidized Bed Reactor," *Engineering*, vol. 5, no. 1, pp. 125–134, 2013, doi: 10.4236/eng.2013.51A018.

[15] A. M. A.-M. Kavin Micheal, A. Ayeshamariam, Rajender Boddula, Prabhakarn Arunachalam, Mohamad S. AlSalhi, J. Theerthagiri, Saradh Prasad, J. Madhavan, "Assembled composite of hematite iron oxide on sponge-like BiOCl with enhanced photocatalytic activity," *Mater. Sci. Energy Technol.*, vol. 2, no. 1, pp. 104–111, 2019, doi: https://doi.org/10.1016/j.mset.2018.11.004.

[16] S.-J. H. Yun Kyung Jo, Jang Mee Lee Son, Suji, "2D inorganic nanosheet-based hybrid photocatalysts: Design, applications, and perspectives," *J. Photochem. Photobiol. C Photochem. Rev.*, vol. 40, pp. 150–190, 2019, doi: https://doi.org/10.1016/j.jphotochemrev.2018.03.002.

[17] L. K. Z. Ye, "A comparative study of photocatalytic activity of ZnS photocatalyst for degradation of various dyes," *Optik (Stuttg).*, vol. 164, pp. 345–354, 2018, doi: https://doi.org/10.1016/j.ijleo.2018.03.030.

[18] R. Saravanan, F. Gracia, and A. Stephen, "Basic Principles, Mechanism, and Challenges of Photocatalysis," *Nanocomposites Visible Light. Photocatal.*, pp. 19–40, 2017, doi: 10.1007/978-3-319-62446-4_2.

[19] M. R. R. Fatemeh Poorsajadi, Mohammad Hossein Sayadi , Mahmood Hajiani, "Photocatalytic degradation of methyl orange dye using bismuth oxide nanoparticles under visible radiation," *Int. J. New Chem.*, vol. 83, pp. 229–239, 2021, doi: 10.22034/ijnc.2020.137235.1131.

[20] B. K. Ali Akbar Isari, Amir Payan, Moslem Fattahi, Sahand Jorfi, "Photocatalytic degradation of rhodamine B and real textile wastewater using Fe-doped TiO2 anchored on reduced graphene oxide (Fe-TiO2/rGO): Characterization and feasibility, mechanism and pathway studies," *Appl. Surf. Sci.*, vol. 462, pp. 549–564, 2018, doi: https://doi.org/10.1016/j.apsusc.2018.08.133.

[21] M. B. K. A.R. Khataee, "Photocatalytic degradation of organic dyes in the presence of nanostructured titanium dioxide: Influence of the chemical structure of dyes," *J. Mol. Catal. A Chem.*, vol. 328, no. 1–2, pp. 8–26, 2010, doi: https://doi.org/10.1016/j.molcata.2010.05.023.

[22] S. M. S. Jorfi, "Visible Light Photocatalytic Degradation of Azo Dye and a Real Textile Wastewater Using Mn, Mo, La/TiO2 /AC Nanocomposite," *Chem. Biochem. Eng. Q.*, 2018, doi: 10.15255/CABEQ.2017.1261.

[23] J. L. Bradshaw, N. Ashoori, M. Osorio, and R. G. Luthy, "Modeling Cost, Energy,

and Total Organic Carbon Trade-Offs for Stormwater Spreading Basin Systems Receiving Recycled Water Produced Using Membrane-Based, Ozone-Based, and Hybrid Advanced Treatment Trains," *Environ. Sci. Technol.*, vol. 53, no. 6, pp. 3128–3139, Mar. 2019, doi: 10.1021/ACS.EST.9B00184.

[24] H. de L. Castrillón, S. Romero-Vargas,Ibrahim, H., "Flow field investigation in a photocatalytic reactor for air treatment (Photo-CREC–air)," *Chem. Eng. Sci.*, vol. 61, no. 10, pp. 3343–3361, 2006, doi: https://doi.org/10.1016/j.ces.2005.11.039.

[25] C. J. C. Cooper Scott, "CFD simulations of particle mixing in a binary fludized bed," *Powder Technol.*, vol. 151, no. 1, pp. 27–36, 2005, doi: 10.1016/j.powtec.2004.11.041.

[26] Y. Jiang, M. R. Khadilkar, M. H. Al-Dahhan, and M. P. Dudukovic, "CFD of multiphase flow in packed-bed reactors: I. k-Fluid modeling issues," *AIChE J.*, vol. 48, no. 4, pp. 701–715, Apr. 2002, doi: 10.1002/AIC.690480406.

[27] W. M. Henk Kaarle Versteeg, "An Introduction to Computational Fluid Dynamics: The Finite Volume Method," Pearson Education Limited. Accessed: Mar. 13, 2025. [Online]. Available: https://books.google.com.pk/books/about/An_Introduction_to_Computational_Fluid_D.html?id=RvBZ-UMpGzIC&redir_esc=y

[28] D. P. P. Iyyapushpam, S., Nishanthi, S.T., "Photocatalytic degradation of methyl orange using α-Bi2O3 prepared without surfactant," *J. Alloys Compd.*, vol. 563, pp. 104–107, 2013, doi: https://doi.org/10.1016/j.jallcom.2013.02.107.

[29] B. Wu, "Computational Fluid Dynamics Investigation of Turbulence Models for Non-Newtonian Fluid Flow in Anaerobic Digesters," *Environ. Sci. Technol.*, vol. 44, no. 23, pp. 8989–8995, Dec. 2010, doi: 10.1021/ES1010016.

[30] David C. Wilcox, "Turbulence Modeling for CFD," *DCW Ind.*, 2006, [Online]. Available: https://cfd.spbstu.ru/agarbaruk/doc/2006_Wilcox_Turbulence-modeling-for-CFD.pdf

[31] A. J. O. et al Ebenezer Oluwatosin Atoyebi, "Computational Fluid Dynamics," *Compr. Mater. Process.*, 2024, [Online]. Available: https://www.sciencedirect.com/topics/materials-science/computational-fluid-dynamics

[32] A. K. Mahdi Ebrahimi Farshchi, Hassan Aghdasinia, "Heterogeneous Fenton reaction for elimination of Acid Yellow 36 in both fluidized-bed and stirred-tank reactors: Computational fluid dynamics versus experiments," *Water Res.*, vol. 151, pp. 203–214, 2019, doi: https://doi.org/10.1016/j.watres.2018.12.011.